Full-symmetry and mixed-symmetry states in even ruthenium isotopes

A. Giannatiempo,[1,2] A. Nannini,[2] P. Sona,[1,2] and D. Cutoiu[3]
[1]*Dipartimento di Fisica, Università di Firenze, Florence, Italy*
[2]*Istituto di Fisica Nucleare, Florence, Italy*
[3]*Department of Heavy Ions Physics, Institute of Atomic Physics, Bucharest, Romania*
(Received 26 July 1995)

The experimental data on positive parity, low-lying levels of the even ruthenium isotopes $^{98-114}$Ru have been analyzed in the framework of the IBA-2 model, with the aim of identifying states having a large mixed-symmetry component. Energies, static and transition electric quadrupole and magnetic dipole moments as well as mixing and branching ratios of the relevant levels have been considered. It appears that the properties of all low-lying levels in these isotopes, for which the comparison between experiment and theory is possible, can be satisfactorily described by the standard IBA-2 model, provided proper account is taken of the presence at low energy of states having a mixed-symmetry character. It seems possible to identify, in each isotope, a few states having such a character, the lowest ones being the 2_3^+ and 3_1^+ levels. Some indications for the presence above the 3_1^+ level of a band of states having $J^\pi=5_1^+,7_1^+,9_1^+$ and a comparable degree of mixed symmetry are pointed out for the heavier nuclei of the chain.

PACS number(s): 21.60.Fw, 21.10.Re, 27.60.+j

I. INTRODUCTION

As all models which distinguish between proton and neutron degrees of freedom, the IBA-2 version of the interacting boson model [1–5] predicts the existence of mixed-symmetry (MS) states, i.e., states not completely symmetric with respect to the proton-neutron boson exchange. A starting point for their identification is provided by the comparison of the experimental excitation energies with those predicted by the model. These depend on the parameters of the adopted Hamiltonian, in particular those appearing in the so called Majorana term. Since no reliable estimate can be given *a priori* of their values (see, e.g., [6]), definite conclusions about the existence of MS states can only be drawn on the basis of their electromagnetic properties which, in the U(5), O(6), and SU(3) limits of the model, are predicted to be quite different from those of fully symmetric (FS) states [7–16]. Indeed, the first definite experimental evidence for the presence of MS states was provided by a particularly high $B(M1)$ strength to the 1^+, 3075 keV state in ^{156}Gd populated via inelastic electron scattering [17].

In the U(5) and O(6) limits of the model the lowest MS state is predicted to have $J^\pi=2^+$ [5]. Evidence for the presence of this state has been found at rather low excitation-energy in several nuclei for which a satisfactory description close to one of these limits can be given (see [18], [19] and references therein). As far as we know, no evidence has yet been found for the presence of MS states having $J^\pi \geqslant 3^+$, except for the 3_1^+ state in ^{200}Hg [20] and no attempt has been made to identify MS states through a systematic investigation along an isotopic chain. Such an analysis, beside providing a much higher confidence on the adopted values of the model parameters, puts the identification of MS states on a sounder basis since the candidates, being states of collective character, must show similar or slowly varying properties along a given isotopic chain or in neighboring chains.

With the aim of identifying states having a large mixed-symmetry component in the mass region $A=100-120$, we have analyzed, in the framework of the IBA-2 model, the isotopic chains of cadmium ($Z=48$) (limited to ^{110,112,114}Cd) [21, 22], palladium ($Z=46$), and ruthenium ($Z=44$) nuclei. In the IBA-2 model space these chains are described as having a number of proton bosons ranging from 1 to 3 and a number of neutron bosons which reaches a maximum of 8 for the neutron number $N=66$, lying midway between the closed shells at $N=50$ and $N=82$. In [21, 22] arguments were given for considering the 2_3^+ level in ^{110,112,114}Cd as the lowest state having a large MS component. In this work we report on the analysis of low-lying positive parity levels in the even isotopes of ruthenium ($^{98-114}$Ru). A similar study concerning palladium ($^{100-116}$Pd) will be the subject of a forthcoming paper.

Preliminary accounts of this work has been presented at the 5th International Spring Seminar at Ravello, 1995 [23].

II. EXCITATION ENERGIES AND PARAMETERS OF THE HAMILTONIAN

The structure of even ruthenium isotopes has been long ago recognized [24], on the basis of an analysis limited to the FS states (IBA-1), as pertaining to the U(5)-O(6) side of the Casten triangle [25]. The only systematic study of the even ruthenium isotopes in the framework of the IBA-2 model has been performed in 1980 by Van Isacker and Puddu [26]. They found an overall good agreement as far as excitation energies and decay properties are concerned, except for the 0_2^+ state in the lighter isotopes, which is supposed to be intruder, and for the 3_1^+ level (the only odd-spin state considered in their work) whose position is systematically predicted too high in energy. The latter disagreement, interpreted by the authors of [26] as a possible indication of a MS state, was ascribed to their choice of the parameters in the Majorana term (see below), which shifts to high energy the MS states. As is well known, these parameters affect the excitation energies of MS states and do not influence those of pure FS states.

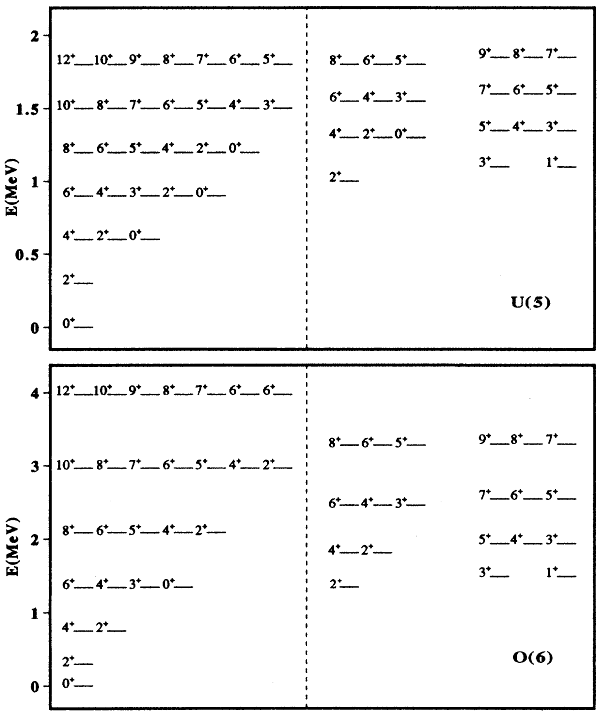

FIG. 1. Excitation-energy pattern of FS states (left-hand side) and of MS states (right-hand side) for the U(5) (upper part) and O(6) (lower part) limits of the IBA-2 model. For the O(6) case only states having the quantum number $\sigma=\sigma_{\max}$ [5] are shown. On the left side degenerate states up to a maximum of six are displayed, starting from the level of highest spin, while on the right part of the figure up to three degenerate levels are shown. For this schematic calculation, performed for a nucleus having $N_\pi=3$ and $N_\nu=4$, the only term used in the Hamiltonian is $\epsilon(\hat{n}_{d_\pi}+\hat{n}_{d_\nu})$, for the U(5) limit, and $\kappa\hat{Q}_\pi\cdot\hat{Q}_\nu$ with $\chi_\pi=\chi_\nu=0$, for the O(6) limit. The values of the coefficients ϵ and κ were chosen as to produce the same energy of the 2_1^+ level in the two cases.

The sizable modification of the excitation-energy pattern which ensues from the presence at low energy of MS states is exemplified, for the case of U(5) and O(6) limits, in Fig. 1. Here FS and MS states are reported on the left and on the right parts of the figure, respectively. The MS states have been further grouped in two columns, the one on the left containing those states which have the same structure as that of the lower-lying FS states of equal spin. The pattern for the two limits is quite similar, both for the FS and MS states, except for a few cases like the 0_2^+ state and its MS counterpart.

For the analysis of excitation energies in ruthenium isotopes we tried to keep to a minimum the number of free parameters in the Hamiltonian. We thus considered equal values for the neutron and proton d-boson excitation-energy ϵ and, in addition to the standard quadrupole interaction and Majorana term, we only considered the dipole neutron-proton boson interaction whose strength is characterized by a single parameter $w_{\pi\nu}$. The explicit expression of the Hamiltonian adopted in the calculations is the following:

$$H=\epsilon(\hat{n}_{d_\pi}+\hat{n}_{d_\nu})+\kappa\hat{Q}_\pi\cdot\hat{Q}_\nu+w_{\pi\nu}\hat{L}_\pi\cdot\hat{L}_\nu+\hat{M}_{\pi\nu}, \quad (1)$$

where the indexes ν and π refer to neutron and proton bosons, respectively, and $\hat{M}_{\pi\nu}$ is the Majorana term. Moreover,

$$\hat{n}_{d_\rho}=(d_\rho^\dagger\cdot\tilde{d}_\rho), \quad (2)$$

$$\hat{Q}_\rho=[d_\rho^\dagger\times\tilde{s}_\rho+s_\rho^\dagger\times\tilde{d}_\rho]^{(2)}+\chi_\rho[d_\rho^\dagger\times\tilde{d}_\rho]^{(2)}, \quad (3)$$

$$\hat{L}_\rho=\sqrt{10}[d_\rho^\dagger\times\tilde{d}_\rho]^{(1)}, \quad (4)$$

$$\hat{M}_{\pi\nu}=\tfrac{1}{2}\,\xi_2[s_\nu^\dagger\times d_\pi^\dagger-s_\pi^\dagger\times d_\nu^\dagger]^{(2)}\cdot[\tilde{s}_\nu\times\tilde{d}_\pi-\tilde{s}_\pi\times\tilde{d}_\nu]^{(2)} - \sum_{k=1,3}\xi_k[d_\nu^\dagger\times d_\pi^\dagger]^{(k)}\cdot[\tilde{d}_\nu\times\tilde{d}_\pi]^{(k)} \quad (\rho=\pi,\nu). \quad (5)$$

In the limiting cases of the IBA-2 model, the F spin is a good quantum number and the FS states are characterized by the eigenvalue $F=F_{\max}=N/2$ (where N is the total number of bosons) while MS states are characterized by $F=F_{\max}-1$, $F_{\max}-2$, etc.

The code NPBOS [27] was used to diagonalize the Hamiltonian. An important quantity contained in its output, for any given state $|s\rangle$, is the ratio R given by

$$R=\frac{\langle s\|F^2\|s\rangle}{F_{\max}(F_{\max}+1)}. \quad (6)$$

In the approximation in which $|s\rangle$ is made out of only two components namely

$$|s\rangle=\alpha|F_{\max}\rangle+\beta|F_{\max}-1\rangle, \quad \alpha^2+\beta^2=1, \quad (7)$$

we have

$$\langle s\|F^2\|s\rangle=\alpha^2F_{\max}(F_{\max}+1)+\beta^2(F_{\max}-1)F_{\max} \quad (8)$$

so that α^2 can be conveniently taken as characterizing the amount of maximum symmetry of the state and as such will be utilized in the following.

To determine the parameters of the Hamiltonian we started from a value of χ_π close to that ($\chi_\pi=-0.8$) we found for cadmium isotopes [21] and from values of χ_ν varying smoothly from -1 in ^{98}Ru to 0 in the heavier isotopes. In each isotope the adjustment of the parameters ϵ, κ, and $w_{\pi\nu}$ was then performed, via an iterative procedure, by exploiting at each step the strong dependence of the energy of the 2_1^+ state on ϵ, of the energy of the even-spin yrast states on k and of the energy splitting of the 0_2^+, 2_2^+, and 4_1^+ levels on $w_{\pi\nu}$. The parameters χ_π and χ_ν have only a minor effect on excitation energies but an important one on the e.m. properties, so that their final choice was made taking also into account their influence on quadrupole moments and $E2/M1$ mixing ratios (see below).

As to the determination of the Majorana parameters, since our main goal in this work was the identification of levels having a large mixed-symmetry component, we adopted different values for ξ_1, ξ_2, and ξ_3 as they affect differently the relevant MS states (see, e.g., [20, 28]). In particular, the

TABLE I. Adopted values for the parameters used for IBA-2 calculations. All parameters are given in MeV except χ_ν (dimensionless). The values $\chi_\pi=-0.8$ and $\xi_1=1.0$ MeV have been chosen for the two parameters, not varied along the isotopic chain.

A	ϵ	k	χ_ν	$w_{\pi\nu}$	ξ_2	ξ_3
98	0.798	−0.06	−1.1	0.010	0.340	−0.270
100	0.791	−0.08	−1.1	0.020	0.295	−0.270
102	0.733	−0.08	−0.4	0.020	0.160	−0.270
104	0.654	−0.09	−0.2	0.020	0.110	−0.240
106	0.574	−0.10	0.0	0.020	0.100	−0.230
108	0.534	−0.10	0.1	0.030	0.050	−0.150
110	0.522	−0.10	0.25	0.035	0.0	−0.120
112	0.463	−0.10	0.4	0.035	0.0	−0.120
114	0.480	−0.10	0.5	0.035	0.0	−0.120

choice $\xi_1 \neq \xi_3$ is suggested by the absence, in all nuclei here examined, of a close doublet of levels having $J^\pi=1^+,3^+$. In fact, by choosing $\xi_1=\xi_3$, such a doublet would be predicted by the model in both the U(5) and O(6) limits. The parameter ξ_1 was fixed at 1 MeV so that the first 1^+ MS state is pushed at an energy $\geqslant 2$ MeV as suggested by the absence, in all the isotopes here examined, of a level having $J^\pi=1^+$ below this energy. We checked also that the position of the levels considered in this work is essentially not affected by the value of ξ_1, when this is varied over quite a large range. The parameters ξ_2, ξ_3 were adjusted so as to reproduce as closely as possible the excitation energy of all positive parity levels for which a clear indication of the spin value exists.

The full set of the Hamiltonian parameters eventually adopted is reported in Table I. It is to be observed (a) the smooth dependence of the parameters on the mass number A; (b) the limited excursion of the parameter κ which remains small all along the isotopic chain, whereas, due to the decreasing ϵ, the ratio κ/ϵ increases monotonically moving toward the neutron midshell, as expected for a structure changing from U(5) to O(6); (c) that the value of χ_ν, varying from large negative values for isotopes at the beginning of the neutron major shell to positive values for isotopes beyond the neutron half shell, shows, as a function of A, the trend expected from microscopic considerations [1]; (d) that the value of χ_ν around the neutron half shell, i.e., for the heavier isotopes, approaches in magnitude the value of χ_π, which fact, as recently noted by Otsuka [30], suggests an O(6) structure for the FS states; (e) the opposite sign of the parameters ξ_2 and ξ_3 and their opposite trend as a function of the neutron-boson number.

In Fig. 2 the calculated excitation patterns for positive parity states in $^{98-114}$Ru are compared to the experimental ones (taken from [31–44]). The calculated data are grouped in two columns according to the values of α^2: states with α^2 larger than 0.5 are reported on the left of the vertical dotted line, the other ones on the right. For each nucleus, all experimental excitation-energies up to the 6_1^+ level are reported. Above this energy, due to the lack of experimental data, the comparison is limited (except for a few cases) to those states having $J^\pi \geqslant 5^+$ for which spin and parity have been either definitely assigned or strongly suggested. The experimental data are also displayed in two columns to help in the comparison with calculated data. It is seen that a remarkably good agreement is obtained all along the isotopic chain.

We stress here a few specific points which appear to be particularly relevant to the main subject of this paper.

(a) The experimental excitation-energy pattern of the even-spin yrast states closely resembles that of the FS states given in Fig. 1, and shows, for increasing mass number, the energy scaling expected for a transition from the U(5) to the O(6) limit. For example, in ^{110}Ru the experimental ratios of the excitation energies of the 4_1^+, 6_1^+, 8_1^+, 10_1^+ levels to that of the 2_1^+ level have the values 2.7, 5.1, 7.9, 11, respectively; these are only about 10% higher than those expected for the O(6) limit. Nuclei at the beginning of the isotopic chain show smaller values for the corresponding ratios, as expected in the U(5) limit.

(b) The excitation energy of the 0_2^+ state is well reproduced all along the isotopic chain. From light to heavy nuclei it increases with respect to the energy of the 2_2^+ and 4_1^+ levels, as expected for a transition from the U(5) to the O(6) limit. Contrary to what claimed by other authors [26, 39], it is therefore unnecessary to introduce configurations lying outside the standard IBA-2 model space to explain the presence of this state at such a low energy. The 0_2^+ state shows a rather pure FS structure all along the chain, since the amount (α^2) of its $F=F_{\max}$ component, which is 0.99 in ^{98}Ru, attains its minimum value 0.79 for ^{114}Ru.

(c) A comparison between the experimental and calculated excitation-energy pattern of FS states (Fig. 1) makes apparent the presence in the former of additional 2^+ states at low energy. Moreover, the presence in the lighter isotopes of two $J^\pi=3^+$ states at an energy close to that of the 6_1^+ state in no way can fit into a scheme restricted to FS states. Indeed, in the pattern shown in Fig. 1, a second 3^+ FS state is predicted at an energy as high as that of the 10_1^+ state.

(d) In both the extreme U(5) and O(6) limits restricted to FS states the 5_1^+, 7_1^+, 9_1^+ levels should be degenerate with the 8_1^+, 10_1^+, 12_1^+ levels, respectively. Instead, the experimental excitation energies of these odd-spin states are systematically lower.

The need for introducing MS states at low energy, by a proper choice of the values of the Majorana parameters, is quite apparent from points (c) and (d). This is further illustrated in Fig. 3 where the calculated energies and $F=F_{\max}$ component of the 3_1^+ and 3_2^+ levels in ^{98}Ru are plotted as a function of ξ_2 and ξ_3. It is seen that the excitation energy of the state having predominant MS character varies almost linearly for increasing ξ_2 or ξ_3, except for a restricted range of

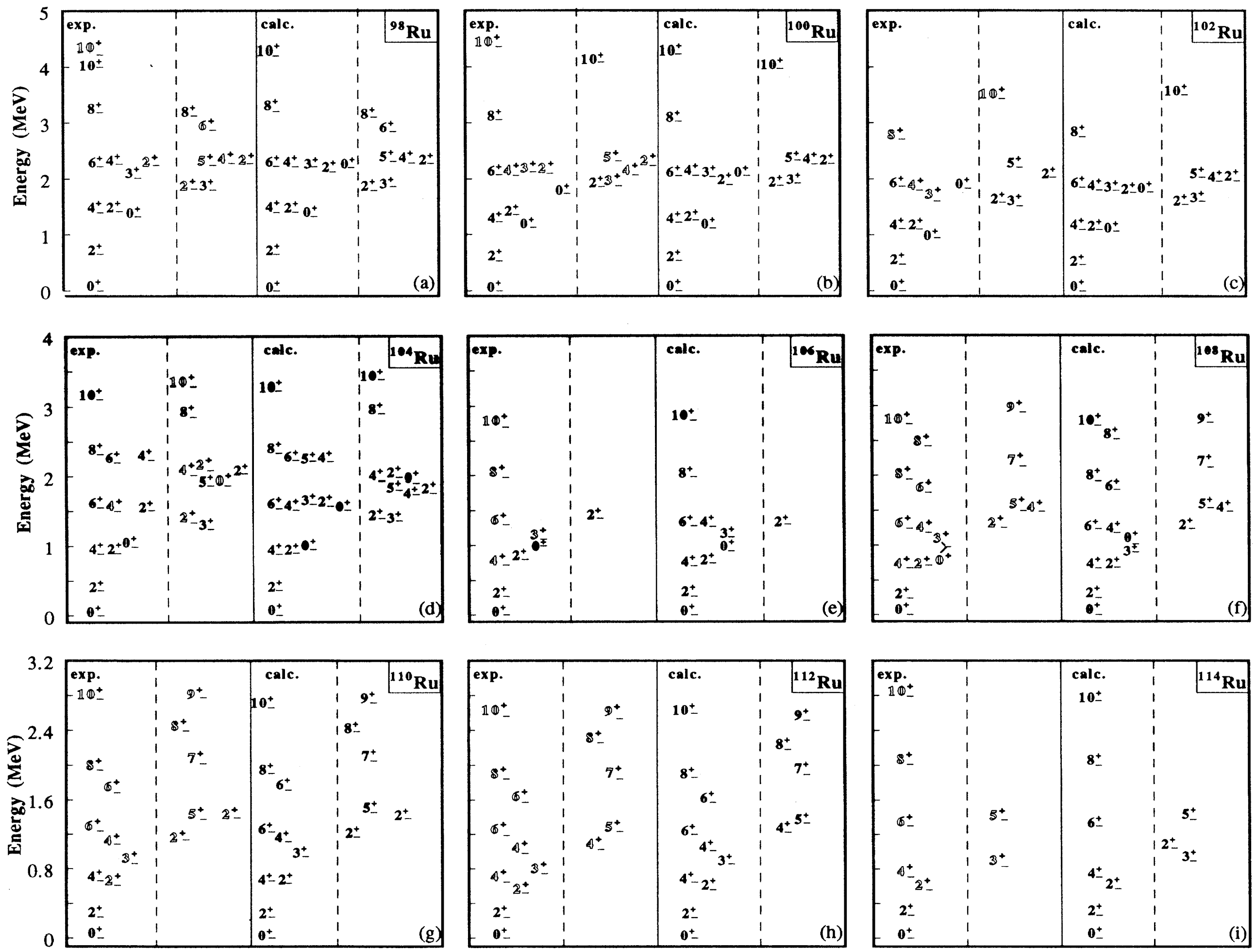

FIG. 2. Experimental and calculated excitation energies for low-lying positive parity states in $^{98-114}$Ru (see text for details). Black numbers in the left part of the figures refer to states whose spin and parity have been definitely assigned.

values of α^2 around 0.5, where level crossing occurs so that the 3^+ state of predominant FS character becomes yrast. Therefore the presence of two 3^+ states at an energy of about 2 MeV can only be accounted for if one of them has basically a MS character.

The decisive importance of the Majorana parameters in achieving satisfactory agreement with the experimental data is illustrated in Fig. 4 where open and solid symbols refer to excitation energies computed for the values of ξ_2 and ξ_3 given in Table I (set I) and for $\xi_2=\xi_3=1$ MeV (set II), respectively. In the latter case the states turn out to have an almost pure FS character. Levels that show a high FS component (α^2) for set I remain at about the same excitation-energy in set II. The reverse however is not generally true, i.e., states that in Fig. 4 appear at about the same energy for the two sets of parameters are not necessarily of FS character. This is because the values of ξ_2 and ξ_3 of set I happen to be close to those for which level crossing occurs (as illustrated in Fig. 3). A striking example is offered by the 2_3^+ level in ^{100}Ru which in set I appears at 1888 keV with a predominant MS character while in set II has an excitation energy of 1904 keV. A similar situation holds for the 8_1^+ state in ^{98}Ru and the 10_1^+ state in ^{100}Ru, which will be discussed in more detail below.

The value of α^2 as a function of the mass number is displayed, for several levels, in Fig. 5. Noteworthy is the high degree of F-spin purity of the states in the lighter isotopes which depends on the smallness of κ/ϵ and $w_{\pi\nu}/\epsilon$ ratios and on the value of χ_ν not being very different from that of χ_π. This leads to a description for these nuclei close to the U(5) limit and makes insignificant the breaking of F-spin symmetry in Hamiltonian (1) due to the absence of $\pi-\pi$ and $\nu-\nu$ quadrupole and dipole interactions with coefficients $\kappa/2$ and $w_{\pi\nu}/2$, respectively.

The F-spin purity of the states decreases towards the neutron midshell but it is still high for yrast high-spin states.

III. ELECTROMAGNETIC PROPERTIES

As shown in the previous section, allowance for the presence of MS states at low energy enabled us to satisfactorily reproduce the excitation energies. A much higher degree of

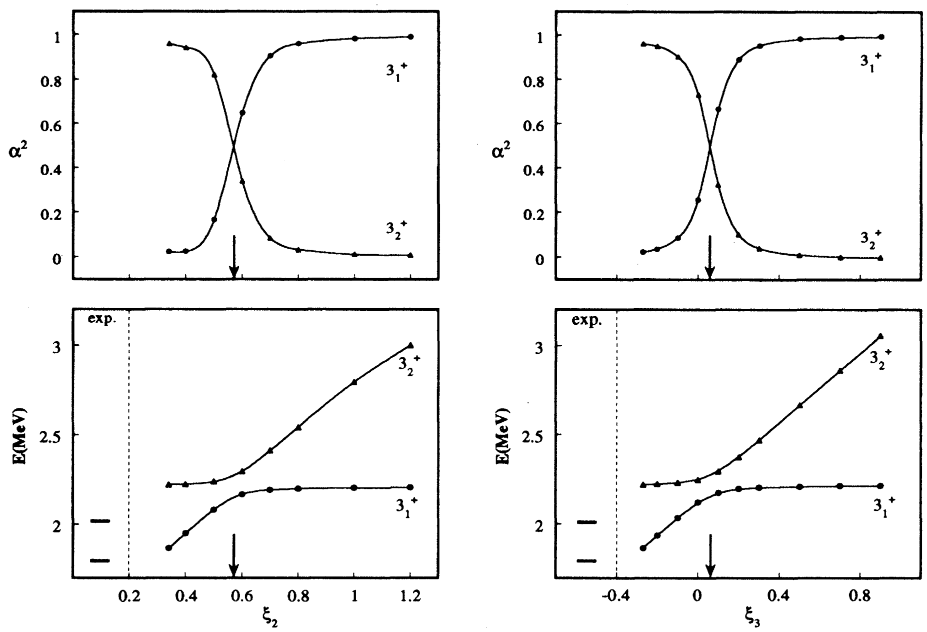

FIG. 3. Calculated energies and full-symmetry component (α^2) of the 3_1^+ and 3_2^+ levels in ^{98}Ru are plotted as a function of the parameter ξ_2 (left) and ξ_3 (right). In each case, the values reported in Table I for the parameters kept fixed have been used. The experimental energies are shown on the left.

confidence in the interpretation proposed in this paper can only be obtained by a comparison of predicted and experimental data on electromagnetic properties.

Signatures for the identification of MS states are related to the matrix elements of the $E2$ and $M1$ operators. In the IBA-2 model their expressions are given by [5]

$$\hat{T}(E2) \equiv e_\pi \hat{T}_\pi(E2) + e_\nu \hat{T}_\nu(E2) = e_\pi \hat{Q}_\pi + e_\nu \hat{Q}_\nu, \quad (9)$$

$$\hat{T}(M1) \equiv g_\pi \hat{T}_\pi(M1) + g_\nu \hat{T}_\nu(M1) = \sqrt{\frac{3}{4\pi}}\,(g_\pi \hat{L}_\pi + g_\nu \hat{L}_\nu), \quad (10)$$

where $\hat{Q}_\rho$ and $\hat{L}_\rho$ are defined in (3) and (4). In (9) and (10) e_ν, e_π and g_ν, g_π have the usual meaning of effective boson charges and g factors.

The main signatures are again most clearly described in the U(5) and O(6) limiting cases of the model. They are well known [7–16] and are based on properties of the transition matrix elements that are briefly recalled hereafter.

(a) Due to the fact that matrix elements $\langle \hat{T}_\pi \rangle$ and $\langle \hat{T}_\nu \rangle$ between states which differ by one unit of F spin have the same absolute values but opposite sign, $E2$ transition probabilities between FS and MS states are as a rule proportional to $(e_\nu - e_\pi)^2$, except for transitions connecting states having the same number of d bosons, in the U(5) limit, which are proportional to $(e_\nu \chi_\nu - e_\pi \chi_\pi)^2$. Indeed, in the latter case only the second term of the quadrupole operator, given in (3), contributes to the transition. As a consequence, $E2$ transitions connecting a FS to a MS state can be strongly reduced with respect to transitions connecting states having the same F spin.

(b) $M1$ transition probabilities are proportional to $(g_\pi - g_\nu)^2$ since the $M1$ operator in (10) can be written as

$$\hat{T}(M1) = \sqrt{\frac{3}{4\pi}}\left[\frac{1}{2}(g_\pi + g_\nu)(\hat{L}_\pi + \hat{L}_\nu) + \frac{1}{2}(g_\pi - g_\nu)(\hat{L}_\pi - \hat{L}_\nu)\right] \quad (11)$$

and only the second term in (11) can have off-diagonal matrix elements, the first one being proportional to the total angular momentum. It can be shown, on the basis of the F-spin formalism, that $M1$ transitions can connect FS states and MS states having $F = F_{\max} - 1$, while they cannot connect FS states (see, e.g., [18]).

To arrive at a comparison as extended as possible between calculated and experimental data we have included in our analysis all available data on electromagnetic properties of the relevant levels, namely, transition and static quadrupole and dipole moments as well as $E2/M1$ mixing ratios and branching ratios.

Of course the analysis must have as a starting point a careful determination of effective boson charges and g factors.

Experimental data on $E2$ reduced transition probabilities and quadrupole moments are given in Table II (which contains all the relevant data reported by Nuclear Data Sheets [31–38] for even ruthenium isotopes) and in Table III (which contains the additional data on ^{104}Ru deduced from [39, 40]). To determine the effective boson charges e_ν and e_π, we considered first the 23 data on $B(E2)$ values reported in Table II, which all refer to transitions between states having almost pure FS character. For each transition the $B(E2)$ value was calculated for different combinations of e_ν and e_π in the range [0.02–0.18 e b]. The result of a minimum χ^2 search in the $e_\nu - e_\pi$ plane [see the contour plot in Fig. 6(a)] shows that, essentially, only the isoscalar combination $e_\nu + e_\pi$ is well determined. This is clearly due to the fact that the neutron and proton $E2$ matrix elements have (except for three

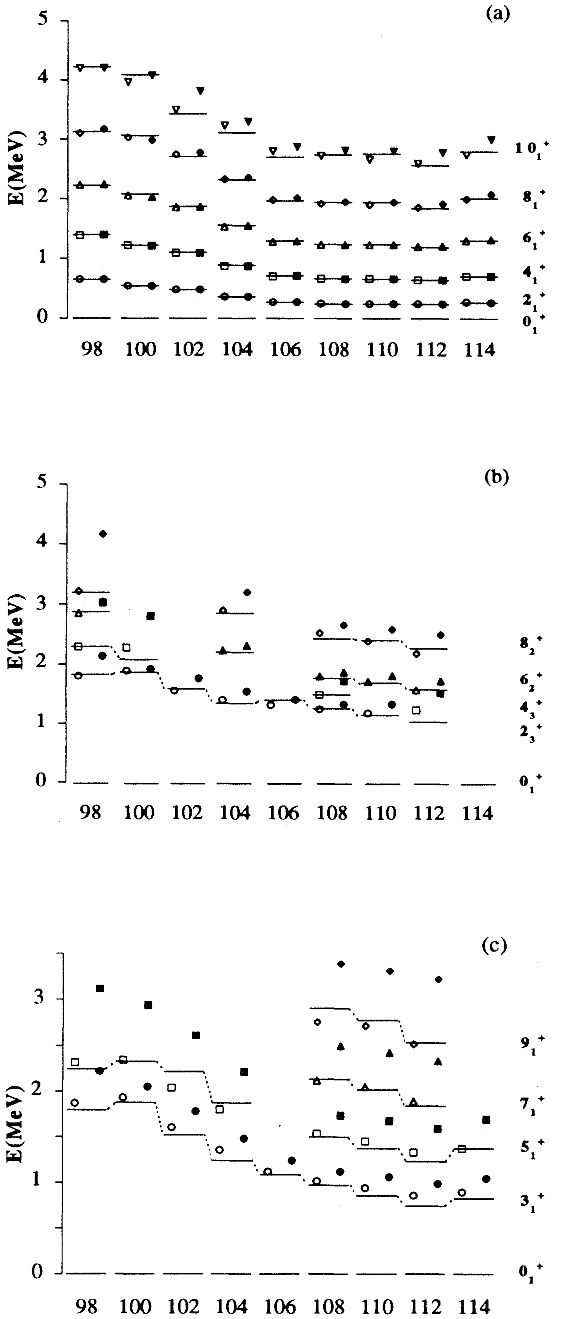

FIG. 4. Experimental (horizontal line) excitation energies in $^{98-114}$Ru are compared with those calculated by using the parameters of Table I (open symbols) and by setting the values of the Majorana parameters ξ_2 and ξ_3 to 1 MeV (solid symbols) for: (a) even-spin yrast states, (b) 2_3^+, 4_3^+, 6_2^+, 8_2^+ states, (c) odd-spin yrast states. In (b) circles, squares, triangles, and diamonds refer to the 2_3^+, 4_3^+, 6_2^+, and 8_2^+ states, respectively. The same symbols in (c) refer to 3_1^+, 5_1^+, 7_1^+, and 9_1^+ states, respectively.

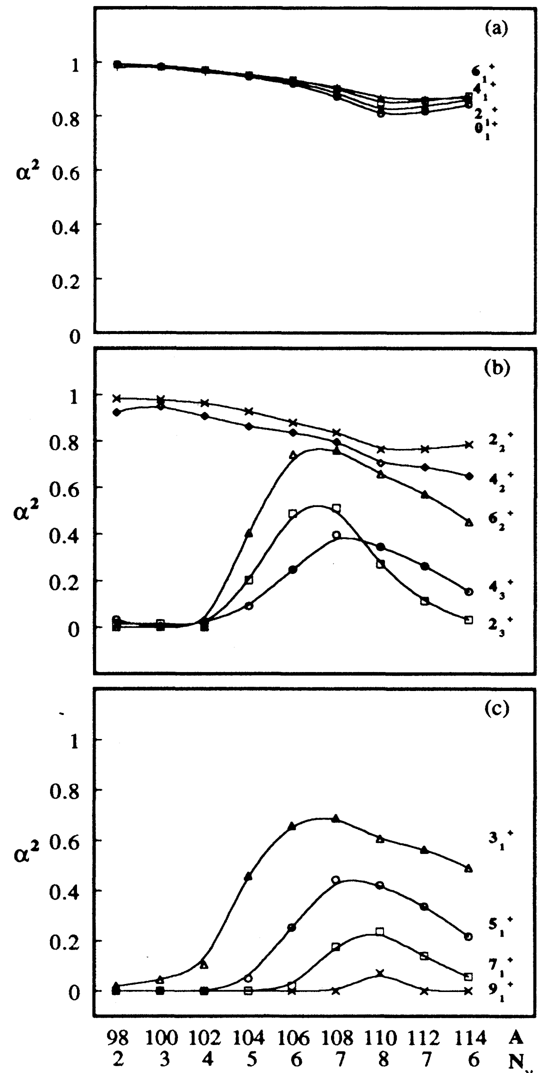

FIG. 5. Amplitude squared of the $F=F_{\max}$ component as a function of the mass number A and number of neutron-boson N_ν for the indicated levels.

cases concerning the $2_2^+ \to 0_1^+$ transition) the same sign. In a similar way, we then considered the 12 experimental data on $E2$ transitions, given in Table III, deexciting the 3_1^+, 4_2^+, 5_1^+, 6_2^+, 8_2^+ states in ^{104}Ru, which, according to the calculations, have a large MS component (except for the 4_2^+ state). The lack of experimental data on such transitions for the other isotopes prevented us from performing a more extended analysis. The contour plot for χ^2 is reported in Fig. 6(b). In this case it is the isovector combination $e_\nu - e_\pi$ which is well determined, due to the fact that for most of the transitions $\langle \hat{T}_\pi \rangle$ and $\langle \hat{T}_\nu \rangle$ have opposite sign. The contour plot obtained by combining all the data is shown in Fig. 6(c). The final choice for the effective boson charges has been $e_\pi = 0.08e$ b, $e_\nu = 0.12e$ b.

By a similar procedure we determined the effective values for g_π and g_ν. The available experimental data, reported in Table IV, are much more limited in this case as we can rely only on four values of magnetic moments and four values of $M1$ reduced transition probabilities. By using only the magnetic moment data we obtain the contour plot for χ^2 in the $g_\pi - g_\nu$ plane given in Fig. 7(a). Here the minimum occurs around $g_\pi \sim 0.4-0.5\mu_N$ and $g_\nu \sim 0.3\mu_N$ and it is essentially the combination $g_\pi + g_\nu$ which is well determined. By con-

TABLE II. Experimental and calculated values for electric quadrupole moments Q (in e b) and reduced transition probabilities $B(E2)$ (in e^2 b^2). The values e_π=0.08 e b and e_ν=0.12 e b for boson effective charges have been used. The experimental data are from [31–38].

A	$Q(2_1^+)$ Expt.	$Q(2_1^+)$ Calc.	$B(E2;0_2^+\to2_1^+)$ Expt.	$B(E2;0_2^+\to2_1^+)$ Calc.	$B(E2;2_1^+\to0_1^+)$ Expt.	$B(E2;2_1^+\to0_1^+)$ Calc.	$B(E2;2_2^+\to0_1^+)$ Expt.	$B(E2;2_2^+\to0_1^+)$ Calc.	$B(E2;2_2^+\to2_1^+)$ Expt.	$B(E2;2_2^+\to2_1^+)$ Calc.	$B(E2;4_1^+\to2_1^+)$ Expt.	$B(E2;4_1^+\to2_1^+)$ Calc.
98	−0.20(9)	−0.30		0.078	0.075(2)	0.057	0.0027(11)	0.0002	0.121(43)	0.069	0.107(16)	0.090
100	−0.46(5)	−0.46	0.097(14)	0.111	0.097(6)	0.087	0.0041(5)	0.0010	0.088(11)	0.081	0.143(11)	0.143
102	−0.68(8)	−0.39	0.099(17)	0.108	0.128(1)	0.114	0.0031(1)	0.0017	0.076(9)	0.133	0.187(28)	0.180
104	−0.70(8)	−0.51	0.073(9)	0.100	0.174(9)	0.158	0.0061(12)	0.0043	0.110(20)	0.159	0.206(38)	0.242
106		−0.65		0.072		0.212		0.0091		0.178		0.314
108		−0.76		0.062	0.214(21)	0.259		0.014		0.193	0.311(24)	0.382
110		−0.80		0.054	0.219(15)	0.297		0.018		0.229		0.439
112		−0.63		0.016	0.225(22)	0.257		0.013		0.242		0.373

sidering also the $B(M1)$ data we obtain the contour plot shown in Fig. 7(b). The minimum of χ^2 occurs at $g_\pi \simeq 0.45\mu_N$ and $g_\nu \simeq 0.35\mu_N$. The slightly modified values $g_\pi = 0.51\mu_N$, $g_\nu = 0.28\mu_N$ have been adopted so as to improve the agreement with experimental data on mixing and branching ratios. Their values are close to those found for this mass region in [21, 45].

Having determined effective charges and g factors, we went on to the final choice of the values of χ_π and χ_ν based, as mentioned above, on a comparison between calculated and experimental data on quadrupole moments and $\delta(E2/M1)$ mixing ratios. The influence of these parameters on δ is due to the small amount of mixing they can induce in states which have basically a FS character, thereby allowing a weak $M1$ component in a transition connecting these states. An example of the constraints on χ_π and χ_ν provided by this comparison is given in Fig. 8 for ^{104}Ru. As seen from Figs. 8(a) and (b) the experimental values of the quadrupole moment of the 2_1^+ state and of the $E2/M1$ mixing ratio $\delta(2_2^+\to2_1^+)$ provide an upper and a lower limit, respectively,

TABLE III. Experimental and calculated values for electric quadrupole moments Q (in e b) and reduced transition probabilities $B(E2)$ (in e^2 b^2) in ^{104}Ru. The values e_π=0.08 e b and e_ν=0.12 e b for boson effective charges have been used. Experimental data are evaluated from [40] except for those marked with the superscript a which are evaluated from [39]. The label 2_4^+ is assigned to the level at 1515 keV (see text).

$J_i^\pi \to J_f^\pi$	Q Expt.	Q Calc.	$B(E2)$ Expt.	$B(E2)$ Calc.
$2_4^+\to0_1^+$			0.0011(13);0.0020(21)[a]	1.3×10^{-5}
$2_4^+\to0_2^+$			0.110(22)[a]	0.071
$2_4^+\to2_1^+$			0.0025(23);0.0047(31)[a]	0.0001
$2_4^+\to2_2^+$			≤0.011(21);0.019(38)[a]	0.023
$2_4^+\to2_4^+$	−0.05(13);−0.52(14)[a]	−0.31		
$2_4^+\to4_1^+$			0.024(31);0.046(50)[a]	0.026
$3_1^+\to2_1^+$			0.0072(6)	0.0086
$3_1^+\to2_2^+$			0.213(35)	0.125
$3_1^+\to4_1^+$			0.046(23)	0.037
$4_1^+\to4_1^+$	−0.32(33)	−0.63		
$4_2^+\to2_1^+$			0.0006(1)	0.0006
$4_2^+\to2_2^+$			0.089(21)	0.128
$4_2^+\to3_1^+$			0.051(7)	0.031
$4_2^+\to4_1^+$			0.055(13)	0.089
$5_1^+\to3_1^+$			0.131(92)	0.118
$6_1^+\to4_1^+$			0.336(28)	0.277
$6_1^+\to6_1^+$	−0.38(15)	−0.65		
$6_2^+\to4_1^+$			$4.9(12)10^{-4}$	1.3×10^{-6}
$6_2^+\to4_2^+$			0.206(29)	0.121
$6_2^+\to6_1^+$			0.059(26)[a]	0.042
$8_1^+\to6_1^+$			0.364(25)	0.280
$8_1^+\to8_1^+$	−0.49(20)	−0.62		
$8_2^+\to6_2^+$			0.245(110)	0.060
$10_1^+\to8_1^+$			0.332(68)	0.225

for the parameter χ_ν. The data also indicate that a value of χ_π around -0.8 is to be preferred. In Fig. 8(c) it is seen how the phases of $\langle T_\pi(M1)\rangle$ [hence the sign of $\delta(2_2^+\to 2_1^+)$] depends on χ_ν.

It was also checked that small variations of χ_π and χ_ν around the values reported in Table I did not produce significant variations on the values of effective charges and g factors obtained through the procedure described above.

The calculated values reported in Tables II–IV are in fairly good agreement with the experimental ones. We note in particular that the magnitude and sign of quadrupole moments as well as $E2$ probabilities for transitions of vastly different intensity originating from the same level are satisfactorily reproduced. The agreement between experimental and computed data for the $0_2^+\to 2_1^+$ transition gives further support to our interpretation of the 0_2^+ state as a state belonging to the IBA-2 model space.

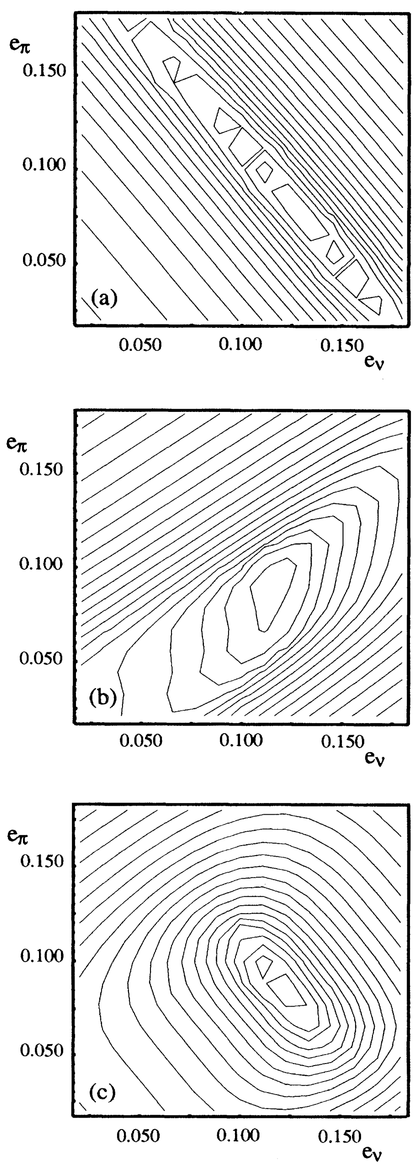

FIG. 6. Contour plot for χ^2 based on the comparison of the computed and experimental data for (a) $B(E2)$ reduced transition probabilities given in Table II, (b) $B(E2)$ of transitions deexciting the 3_1^+, 4_2^+, 5_1^+, 6_2^+, and 8_2^+ states in ^{104}Ru, given in Table III, (c) the combined data.

The experimental and calculated data for $E2/M1$ mixing ratios and branching ratios are given in Tables V and VI. In the latter, for every transition we report the energy and the calculated values for $B(M1)$, $B(E2)$ and the absolute transition probabilities $W_\gamma(M1)$ and $W_\gamma(E2)$, deduced via the expressions

$$W_\gamma(M1)=1.76\ \ 10^{13}E_\gamma^3(\mathrm{MeV})B(M1)\ \ \mathrm{s}^{-1}, \quad (12)$$

$$W_\gamma(E2)=1.22\ \ 10^{13}E_\gamma^5(\mathrm{MeV})B(E2)\ \ \mathrm{s}^{-1}. \quad (13)$$

The relative importance of the $M1$ and $E2$ component in determining the branching ratios is thereby clearly visible.

As far as the mixing ratios are concerned, we first observe that the calculations are able to reproduce the absolute values and the change in sign of $\delta(2_2^+\to 2_1^+)$ between ^{100}Ru and ^{102}Ru but not that between ^{104}Ru and ^{106}Ru. This is related to the dependence of $\langle \hat{T}_\pi(M1;2_2^+\to 2_1^+)\rangle$ on the parameter χ_ν which shows, in each isotope, a trend similar to that given in Fig. 8(c) for ^{104}Ru. It is found that $\langle \hat{T}_\pi(M1)\rangle$ (hence δ) changes sign with respect to $\langle \hat{T}(E2)\rangle$ when the condition $\chi_\nu N_\pi=\chi_\pi N_\nu$ is approximately satisfied. In ^{100}Ru $|\chi_\nu|N_\pi$ is larger than $|\chi_\pi|N_\nu$ and vice versa in ^{102}Ru. An unreasonably low value of χ_ν ($\chi_\nu<-1.2$) would be required to allow for the change in sign from ^{104}Ru to ^{106}Ru, so that, at present, the contradiction with the experimental data appears inexplicable. On the other hand for the adopted values of χ_ν the branching ratio $W_\gamma(2_2^+\to 0_1^+)/W_\gamma(2_2^+\to 2_1^+)$ is predicted to be 0.41, 0.59, 0.92, 1.07 in ^{106,108,110,112}Ru, respectively which compares well with the corresponding experimental value 0.69 (7), 0.80 (6), 0.94 (7), 0.82 ([35, 37, 38, 42]).

IV. EVIDENCE FOR MS STATES FROM e.m. PROPERTIES

We now analyze the data of Tables V and VI from the point of view of what support they provide, if any, to our interpretation of some of the levels as having a large MS component.

A. Even-spin states

We discuss first even-spin states starting from the 2_3^+ level, on which some preliminary comments are in order. In ^{100}Ru we have recently identified this level with the one at 1865 keV by means of internal conversion coefficient measurements [44]. In ^{104}Ru Stachel *et al.* [39, 40] consider the 0_2^+ state at 988 keV as a state outside the IBA-2 model space (contrary to what we claim in this work), and propose the assignment $J^\pi=0^+$ to the level at 1335 keV which they interpret as the lowest 0^+ state of collective nature. We instead propose for this level, which is observed to decay only to the 2_1^+ level, spin-parity $J^\pi=2^+$, so that it would become the third excited state of such a spin, while the well established $J^\pi=2^+$ level at 1515 keV would become the fourth one. Our proposal is based both on the results of the calculations, which predict the existence of two $J^\pi=2^+$ levels in the 1300–1500 keV excitation-energy range, and on the analogy with the properties of the 2_3^+ level in the neighboring isotopes ^{102,106}Ru, where this state decays with the strongest

TABLE IV. Experimental and calculated values of magnetic dipole moments μ (in μ_N) and reduced transition probabilities $B(M1)$ (in μ_N^2). The values $g_\pi = 0.51\mu_N$, $g_\nu = 0.28\mu_N$ for the effective g factors have been used. The label 2_4^+ is assigned to the level at 1515 keV (see text). Experimental data are from [31–34, 39].

	$\mu(2_1^+)$		$B(M1;2_2^+\to 2_1^+)$		$B(M1;2_4^+\to 2_1^+)$	
A	Expt.	Calc.	Expt.	Calc.	Expt.	Calc.
98	0.80(60)	0.81	$3(2)\times 10^{-4}$	1×10^{-4}		
100	0.94(12)	0.79	$36(18)\times 10^{-4}$	2×10^{-5}		
102	0.71(6)	0.77				
104	0.82(10)	0.76	$3(1)\times 10^{-4}$	3×10^{-4}	$23(20)\times 10^{-3}$	3×10^{-3}

branch to the 2_1^+ level. In any case it would be desirable to perform a new experiment to resolve the issue.

As to ^{110}Ru, on the basis of the calculated energies, we suggest that the level at 1137 keV (proposed in [38]) is to be identified with the 2_3^+ state.

As follows from what has been said above about the decay properties of MS states in nuclei having a structure close to the U(5) or O(6) limit, the lowest 2^+ MS state is characterized by a decay to the 2_1^+ level through a transition dominated by its $M1$ component, thus implying a rather small value of δ (see, e.g., [18]). This is indeed what is observed for the $2_3^+\to 2_1^+$ transition in the few isotopes (^{102,106,108}Ru) for which the mixing ratio has been measured (see Table V).

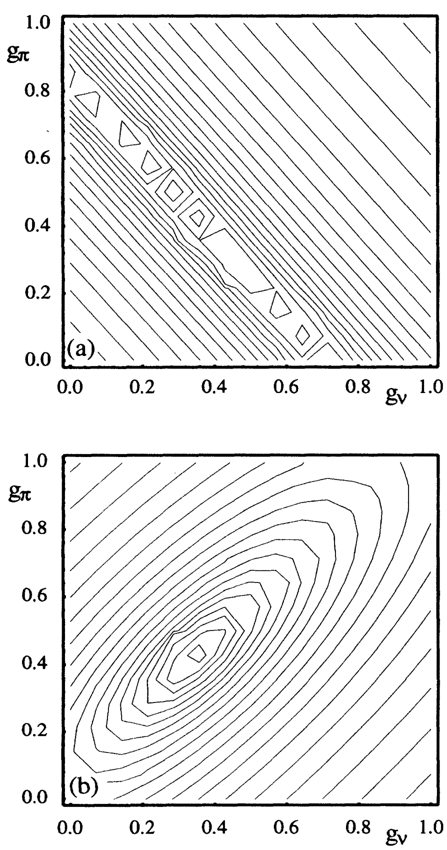

FIG. 7. Contour plot for χ^2 based on the comparison of the computed and experimental data for (a) dipole magnetic moments, (b) all the data given in Table IV.

In the isotopes ^{98,100,102}Ru, which have a structure close to the U(5) limit, further evidence favoring the interpretation of the 2_3^+ state as one characterized by a large MS component is provided by the very similar values observed for the $\log ft$ of the Gamow-Teller $\beta^\pm$ transitions connecting the ground state of the odd-odd adjacent isobars ($J^\pi = 1^+, 2^+$) to the 2_1^+ and 2_3^+ states. Indeed, as explained in detail in [46], in the U(5) limit the even-even core of the ground state of the parent nucleus should be described by the boson configuration $s_\pi^{N\pi} s_\nu^{N\nu}$ while, in the simplest interpretation, the spin parity $J^\pi = 1^+, 2^+$ would result from the coupling $(\pi g_{9/2} \otimes \nu g_{7/2})^{1,2}$ of the odd nucleons. The GT decay to the 2_1^+ and 2_3^+ states, induced by the transition $\nu g_{7/2}\to \pi g_{9/2}$ or $\pi g_{9/2}\to \nu g_{7/2}$, leads to the configuration $(\pi g_{9/2}\otimes \pi g_{9/2})^2$ or $(\nu g_{7/2}\otimes \nu g_{7/2})^2$ which is a component of a proton or neutron d-boson, respectively. In the U(5) limit the wave functions of the $1d$-boson FS and MS state are given, in a shorthand notation, by [11]

$$|\psi_{\mathrm{FS}}\rangle = \sqrt{\frac{N_\pi}{N}}\,|s_\pi^{N\pi-1} s_\nu^{N\nu} d_\pi\rangle + \sqrt{\frac{N_\nu}{N}}\,|s_\pi^{N\pi} s_\nu^{N\nu-1} d_\nu\rangle, \tag{14}$$

$$|\psi_{\mathrm{MS}}\rangle = \sqrt{\frac{N_\nu}{N}}\,|s_\pi^{N\pi-1} s_\nu^{N\nu} d_\pi\rangle - \sqrt{\frac{N_\pi}{N}}\,|s_\pi^{N\pi} s_\nu^{N\nu-1} d_\nu\rangle. \tag{15}$$

Clearly, the GT operator connects the parent state only to the first component of the wavefunction in β^- decay and to the second component in β^+ decay so that the values of $\log ft$ to the FS and MS 2^+ states should only differ by the quantity $\log(N_\pi/N_\nu)$. The relevant data for the $\beta^\pm$ decay to the three lowest 2^+ levels in ^{98,100,102}Ru are given in Table VII. For these isotopes $\log(N_\pi/N_\nu)$ amounts to 0.18, 0, −0.12, respectively. The very close experimental values of $\log ft$ for the transitions to the 2_1^+, 2_3^+ states confirm the interpretation of the latter as essentially a $1d$-boson MS state. Instead, a $3d$-boson interpretation (corresponding to the third 2^+ FS state) would imply a $\log ft$ certainly larger than that pertaining to the 2_2^+ state, which is basically a $2d$-boson state.

Detailed comparison of calculated and experimental values for the $\log ft$ values in even ruthenium and palladium isotopes (in addition to those reported in [46]) will be reported elsewhere.

Even the comparison of the experimental and calculated values for the branching ratios from the 2_3^+ level strengthens our confidence in the proposed interpretation. Note that the

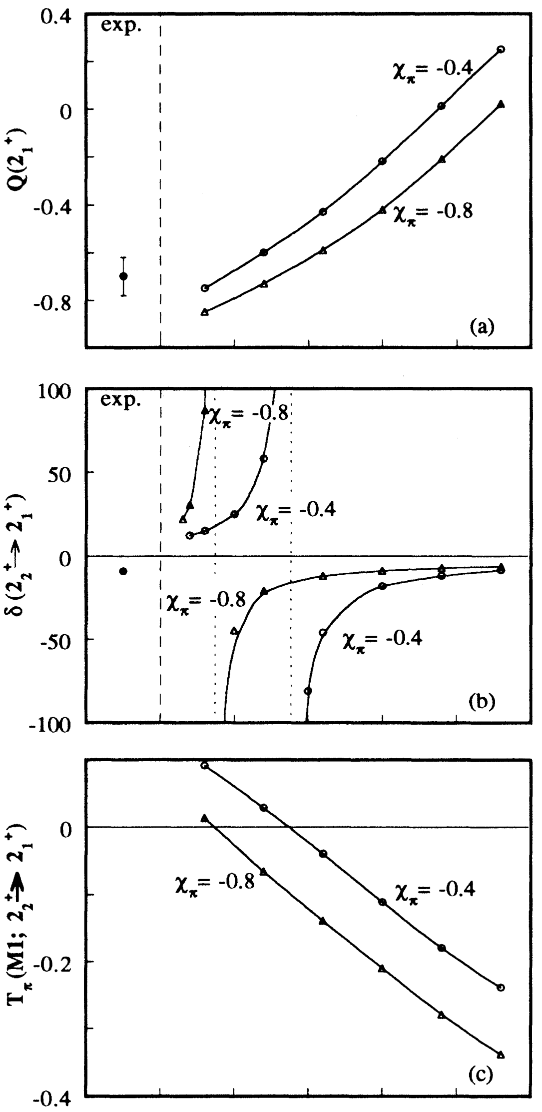

FIG. 8. Calculated values of the (a) electric quadrupole moment of the 2_1^+ level, (b) $E2/M1$ mixing ratio for the transition $2_2^+ \to 2_1^+$, (c) reduced $M1$ neutron matrix element for the same transition, as a function of χ_ν, for two values of χ_π, in ^{104}Ru. The remaining Hamiltonian parameters are those given in Table I. In (c) positive sign has been taken for $\langle \hat{T}_\pi(M1)\rangle$ [which is opposite $\langle \hat{T}_\nu(M1)\rangle$] when its phase is the same as that of $\langle \hat{T}(E2)\rangle$. The vertical dotted lines mark the inversion of sign of δ, corresponding to that of $\langle \hat{T}_\pi(M1)\rangle$, for the different χ_π values. Experimental data are given on the left of (a) and (b); in the latter the size of the dot is larger than the error bar.

reasonable agreement results, according to the calculated values given in columns 6 and 7 of Table VI, from the $2_3^+ \to 2_1^+$ transition being dominated by its $M1$ component and the remaining deexciting transitions by their $E2$ component.

As a final remark we note that the intensity ratio $S = W_\gamma(2_3^+ \to 0_1^+)/W_\gamma(2_3^+ \to 2_1^+)$ is particularly sensitive, in the heavier isotopes, to the presence of a large MS component. Indeed, if quite pure FS wave functions had been used,

TABLE V. Experimental and calculated values for the $E2/M1$ mixing ratios δ (in MeV e b/μ_N). Experimental values are from [31–36].

A	$J_i^\pi \to J_f^\pi$	δ_{expt}	$\delta_{\text{calc.}}$
98	$2_2^+ \to 2_1^+$	13(4)	15
100	$2_2^+ \to 2_1^+$	3.2(8)	43
102	$2_2^+ \to 2_1^+$	$-60(20)$	-16
104	$2_2^+ \to 2_1^+$	$-9(2)$	-10
106	$2_2^+ \to 2_1^+$	$7.1^{+1.6}_{-1.1}$	-9
108	$2_2^+ \to 2_1^+$	$4.3^{+0.9}_{-0.6}$	-7
102	$2_3^+ \to 2_1^+$	0.25(3)	0.11
106	$2_3^+ \to 2_1^+$	$0.24^{+0.13}_{-0.12}$	0.43
108	$2_3^+ \to 2_1^+$	$0.9^{+0.7}_{-0.5}$	0.6
104	$2_4^+ \to 2_1^+$	0.4(1)	0.2
98	$3_1^+ \to 2_1^+$	<-0.2	-1.5
102	$3_1^+ \to 2_1^+$	$-5.7(3)$	-2.2
104	$3_1^+ \to 2_1^+$	$-3.2(4)$	-2.9
106	$3_1^+ \to 2_1^+$	$-3.8^{+0.9}_{-1.6}$	-4.4
108	$3_1^+ \to 2_1^+$	$-3.0^{+0.7}_{-1.4}$	-4.6
98	$3_1^+ \to 2_2^+$	$0.4^{+1.7}_{-0.3}$	0.3
102	$3_1^+ \to 2_2^+$	$-7.2(10)$	-0.6
102	$5_1^+ \to 4_1^+$	$-1.1^{+0.6}_{-0.9}$	-1.2

like those one would obtain by choosing $\xi_1 = \xi_2 = \xi_3 = 1$ MeV in the Hamiltonian (1), the values $S = 80$, 59 would have been obtained in ^{106,108}Ru, to be compared with experimental values 0.23(4), 0.67(11), respectively.

We now consider the 2_4^+ state which, according to the calculations, should have a noticeable MS component in the isotopes with $A \geqslant 104$. Unfortunately, almost nothing is known about the location of the 2_4^+ state; the only exception is possibly to be found in ^{104}Ru. Indeed, if, as mentioned above, the level at 1515 keV in this nucleus is to be identified with the 2_4^+ state, the model predictions are seen to be quite reasonable by comparing experimental and calculated values for $B(E2)$'s and branching ratios of the transitions deexciting this level and for the mixing ratio $\delta(2_4^+ \to 2_1^+)$ (see Tables III, V, and VI). We stress the importance, for this comparison, of the presence in the $2_4^+ \to 2_1^+$ transition of a strong $M1$ component which directly reflects the MS content of the wave function describing the 2_4^+ level.

As to the identification of the low-lying states with $J^\pi = 4^+, 6^+, 8^+, 10^+$ having a large MS component, the calculations suggest that they should be identified with the 4_3^+, 6_2^+, 8_2^+ states, respectively, in the whole isotopic chain and with the 10_1^+ state in ^{100,102}Ru. Experimentally, in none of the isotopes the 4_3^+ level has been definitely identified. The 6_2^+ and 8_2^+ states have been identified or strongly suggested in ^{98,104,108,110,112}Ru while the 10_1^+ state has been established in all isotopes of the chain. The decay properties of the 6_2^+ level, whose MS component $(1-\alpha^2)$ is seen in Fig. 5, are reasonably reproduced by the calculations (see Tables III and VI). As to the states of spin $J = 8,10$, particularly interesting is the case of ^{98}Ru. In this nucleus there is a doublet of levels at 3126 and 3190 keV for which the assignment $J^\pi = 8^+$ has been definitely established and two levels are found at 4001 and 4223 keV, the assignment $J^\pi = 10^+$ being definite for the former and suggested for the latter. According to the calcu-

TABLE VI. Experimental and calculated branching ratios for γ transitions deexciting indicated levels in $^{98-112}$Ru. Contributions from internal conversion electrons are negligible and have not been considered. The units for the energy E_γ, the $B(M1)$ and the $B(E2)$ are MeV, μ_N^2 and $e^2\,b^2$, respectively. The absolute $M1$ and $E2$ transition probabilities (in 10^{13} s^{-1}) are given in columns 6 and 7. Experimental values are from [31–38] apart from those marked by the superscript a which are taken from [42].

A	$J_i^\pi \to J_f^\pi$	E_γ	$B(M1)$	$B(E2)$	$W_\gamma(M1)$	$W_\gamma(E2)$	Branching ratio Calc.	Expt.
98	$2_3^+\to 0_1^+$	1.817	0	1.45×10^{-3}	0	3.50×10^{-2}	71	104(10)
	$2_3^+\to 2_1^+$	1.165	1.75×10^{-2}	1.16×10^{-4}	4.88×10^{-2}	3.03×10^{-4}	100	100(7)
	$3_1^+\to 2_1^+$	1.144	3.70×10^{-4}	9.79×10^{-4}	9.75×10^{-4}	2.34×10^{-3}	100	100(7)
	$3_1^+\to 2_2^+$	0.383	1.17×10^{-2}	9.09×10^{-3}	1.16×10^{-3}	9.14×10^{-5}	38	26(1)
	$3_1^+\to 4_1^+$	0.399	8.95×10^{-3}	3.68×10^{-3}	1.00×10^{-3}	4.54×10^{-5}	31	7(1)
	$8_1^+\to 6_1^+$	0.904	0	3.46×10^{-2}	0	2.55×10^{-2}	100	100
	$8_1^+\to 6_2^+$	0.259	0	6.00×10^{-4}	0	8.53×10^{-7}	0	-
	$8_2^+\to 6_1^+$	0.968	0	5.24×10^{-2}	0	5.43×10^{-2}	100	100
	$8_2^+\to 6_2^+$	0.323	0	4.00×10^{-4}	0	1.72×10^{-6}	0	-
	$10_2^+\to 8_1^+$	1.096	0	1.90×10^{-2}	0	3.67×10^{-2}	74	85(7)
	$10_2^+\to 8_2^+$	1.033	0	3.47×10^{-2}	0	4.98×10^{-2}	100	100(7)
100	$2_3^+\to 0_1^+$	1.865	0	1.11×10^{-3}	0	3.04×10^{-2}	100	100(12)
	$2_3^+\to 0_2^+$	0.735	0	1.06×10^{-2}	0	2.77×10^{-3}	9	100(12)
	$2_3^+\to 2_1^+$	1.325	1.35×10^{-2}	2.59×10^{-4}	5.53×10^{-2}	1.29×10^{-3}	186	86(10)
	$2_3^+\to 2_2^+$	0.503	8.00×10^{-4}	7.29×10^{-3}	1.79×10^{-4}	2.86×10^{-4}	2	18(3)
	$2_3^+\to 4_1^+$	0.639	0	7.49×10^{-3}	0	9.74×10^{-4}	3	22(3)
	$3_1^+\to 2_1^+$	1.341	1.00×10^{-3}	5.73×10^{-4}	4.24×10^{-3}	3.03×10^{-3}	100	100(5)
	$3_1^+\to 2_2^+$	0.519	1.02×10^{-2}	1.19×10^{-2}	2.51×10^{-3}	5.46×10^{-4}	42	22(7)
	$3_1^+\to 4_1^+$	0.655	7.99×10^{-3}	3.88×10^{-3}	3.95×10^{-3}	5.71×10^{-4}	62	13(4)
102	$2_3^+\to 0_1^+$	1.581	0	2.02×10^{-3}	0	2.43×10^{-2}	64	11(2)
	$2_3^+\to 0_2^+$	0.637	0	3.82×10^{-3}	0	4.89×10^{-4}	1	57(5)
	$2_3^+\to 2_1^+$	1.106	1.58×10^{-2}	2.09×10^{-4}	3.75×10^{-2}	4.21×10^{-4}	100	100(7)
	$2_3^+\to 2_2^+$	0.477	5.07×10^{-4}	4.01×10^{-6}	9.69×10^{-5}	1.21×10^{-7}	0.3	-
	$2_3^+\to 4_1^+$	0.475	0	1.56×10^{-3}	0	4.59×10^{-5}	0.1	-
	$3_1^+\to 2_1^+$	1.047	9.07×10^{-4}	4.13×10^{-3}	1.83×10^{-3}	6.34×10^{-3}	100	100(4)
	$3_1^+\to 2_2^+$	0.418	1.30×10^{-2}	2.83×10^{-2}	1.68×10^{-3}	4.43×10^{-4}	26	32(2)
	$3_1^+\to 4_1^+$	0.415	1.27×10^{-2}	8.55×10^{-3}	1.60×10^{-3}	1.29×10^{-4}	21	6.2(5)
	$5_1^+\to 3_1^+$	0.697	0	1.01×10^{-1}	0	2.03×10^{-2}	100	100(6)
	$5_1^+\to 4_1^+$	1.113	1.83×10^{-3}	2.19×10^{-3}	4.40×10^{-3}	4.50×10^{-3}	43	42(3)
	$5_1^+\to 4_2^+$	0.420	1.54×10^{-2}	8.06×10^{-3}	2.01×10^{-3}	1.29×10^{-4}	10	7(1)
	$5_1^+\to 6_1^+$	0.346	2.15×10^{-2}	2.44×10^{-3}	1.57×10^{-3}	1.48×10^{-5}	7	1.9(2)
104	$2_4^+\to 0_1^+$	1.515	0	1.31×10^{-5}	0	1.27×10^{-4}	2	28(3)
	$2_4^+\to 0_2^+$	0.527	0	7.06×10^{-2}	0	3.50×10^{-3}	45	14(3)
	$2_4^+\to 2_1^+$	1.157	2.80×10^{-3}	7.13×10^{-5}	7.64×10^{-3}	1.81×10^{-4}	100	100(9)
	$2_4^+\to 4_1^+$	0.627	0	2.60×10^{-2}	0	3.07×10^{-3}	39	8(2)
	$3_1^+\to 2_1^+$	0.884	5.70×10^{-4}	8.57×10^{-3}	6.94×10^{-4}	5.66×10^{-3}	100	100(13)
	$3_1^+\to 2_2^+$	0.349	5.30×10^{-3}	1.25×10^{-1}	3.98×10^{-4}	7.92×10^{-4}	19	23(2)
	$3_1^+\to 4_1^+$	0.354	4.09×10^{-3}	3.70×10^{-2}	3.19×10^{-4}	2.50×10^{-4}	9	9(2)
	$5_1^+\to 3_1^+$	0.630	0	1.18×10^{-1}	0	1.43×10^{-2}	100	100(40)
	$5_1^+\to 4_1^+$	0.984	1.65×10^{-3}	3.17×10^{-3}	2.77×10^{-3}	3.57×10^{-3}	44	34(6)
106	$2_3^+\to 0_1^+$	1.392	0	1.57×10^{-3}	0	1.00×10^{-2}	69	23(3)
	$2_3^+\to 0_2^+$	0.401	0	8.89×10^{-2}	0	1.12×10^{-3}	8	7(3)
	$2_3^+\to 2_1^+$	1.122	4.94×10^{-3}	1.02×10^{-3}	1.23×10^{-2}	2.22×10^{-3}	100	100(10)
	$2_3^+\to 2_2^+$	0.600	3.78×10^{-4}	4.12×10^{-3}	1.44×10^{-4}	3.91×10^{-4}	4	-
	$2_3^+\to 4_1^+$	0.677	0	1.77×10^{-2}	0	3.08×10^{-3}	21	23(3)
	$3_1^+\to 2_1^+$	0.821	3.80×10^{-4}	1.53×10^{-2}	3.70×10^{-4}	6.98×10^{-3}	100	100(11)
	$3_1^+\to 2_2^+$	0.299	2.96×10^{-3}	2.31×10^{-1}	1.40×10^{-4}	6.75×10^{-4}	11	17(6)
	$3_1^+\to 4_1^+$	0.377	2.19×10^{-3}	6.64×10^{-2}	2.07×10^{-4}	6.17×10^{-4}	11	11(6)
108	$2_3^+\to 0_1^+$	1.249	0	1.74×10^{-3}	0	6.47×10^{-3}	50	67(11)
	$2_3^+\to 0_2^+$	0.273	0	1.20×10^{-1}	0	2.22×10^{-4}	2	11(3)
	$2_3^+\to 2_1^+$	1.007	5.53×10^{-3}	2.33×10^{-3}	9.94×10^{-3}	2.94×10^{-3}	100	100(4)
	$2_3^+\to 2_2^+$	0.541	1.65×10^{-4}	2.00×10^{-3}	4.61×10^{-5}	1.13×10^{-4}	1	15(2)
	$2_3^+\to 4_1^+$	0.584	0	1.98×10^{-2}	0	1.64×10^{-3}	13	28(9)
	$3_1^+\to 2_1^+$	0.733	4.10×10^{-4}	2.31×10^{-2}	2.84×10^{-4}	5.97×10^{-3}	100	100(8)

TABLE VI. (*Continued.*)

A	$J_i^\pi \rightarrow J_f^\pi$	E_γ	$B(M1)$	$B(E2)$	$W_\gamma(M1)$	$W_\gamma(E2)$	Branching ratio Calc.	Expt.
	$3_1^+ \rightarrow 2_2^+$	0.267	2.43×10^{-3}	3.09×10^{-1}	8.14×10^{-5}	5.12×10^{-4}	10	11(2)
	$3_1^+ \rightarrow 4_1^+$	0.310	1.83×10^{-3}	8.58×10^{-2}	9.60×10^{-5}	3.00×10^{-4}	6	6(1)
	$5_1^+ \rightarrow 3_1^+$	0.522	0	2.33×10^{-1}	0	1.10×10^{-2}	100	100[a]
	$5_1^+ \rightarrow 4_1^+$	0.832	1.20×10^{-3}	7.84×10^{-3}	1.22×10^{-3}	3.81×10^{-3}	46	47[a]
	$5_1^+ \rightarrow 4_2^+$	0.314	4.40×10^{-3}	1.15×10^{-1}	2.40×10^{-4}	4.30×10^{-4}	6	10.7[a]
	$6_2^+ \rightarrow 4_1^+$	1.097	0	9.64×10^{-5}	0	1.87×10^{-4}	0.8	-
	$6_2^+ \rightarrow 4_2^+$	0.579	0	2.99×10^{-1}	0	2.37×10^{-2}	100	100[a]
	$6_2^+ \rightarrow 5_1^+$	0.265	2.00×10^{-5}	1.86×10^{-2}	6.55×10^{-7}	2.96×10^{-5}	0.1	-
	$7_1^+ \rightarrow 5_1^+$	0.637	0	3.09×10^{-1}	0	3.96×10^{-2}	100	100[a]
	$7_1^+ \rightarrow 6_1^+$	0.893	2.20×10^{-3}	1.81×10^{-3}	2.76×10^{-3}	1.25×10^{-3}	10	-
	$7_1^+ \rightarrow 6_2^+$	0.372	7.10×10^{-3}	5.61×10^{-2}	6.43×10^{-4}	4.88×10^{-4}	3	-
	$8_2^+ \rightarrow 6_1^+$	1.180	0	4.82×10^{-4}	0	1.35×10^{-3}	3	-
	$8_2^+ \rightarrow 6_2^+$	0.659	0	3.00×10^{-1}	0	4.55×10^{-2}	100	100[a]
	$9_1^+ \rightarrow 7_1^+$	0.777	0	3.45×10^{-1}	0	1.19×10^{-1}	100	100[a]
	$9_1^+ \rightarrow 8_1^+$	0.968	3.11×10^{-3}	1.03×10^{-4}	4.96×10^{-3}	1.07×10^{-4}	4	-
	$9_1^+ \rightarrow 8_2^+$	0.489	1.58×10^{-2}	3.53×10^{-2}	3.25×10^{-3}	1.21×10^{-3}	4	-
	$9_1^+ \rightarrow 10_1^+$	0.171	1.95×10^{-2}	2.81×10^{-2}	1.72×10^{-4}	5.01×10^{-6}	0.1	-
	$10_1^+ \rightarrow 8_1^+$	0.797	0	4.36×10^{-1}	0	1.71×10^{-1}	100	100[a]
	$10_1^+ \rightarrow 8_2^+$	0.318	0	1.85×10^{-3}	0	7.36×10^{-6}	0	-
110	$3_1^+ \rightarrow 2_1^+$	0.619	5.50×10^{-4}	2.87×10^{-2}	2.30×10^{-4}	3.19×10^{-3}	100	100(7)
	$3_1^+ \rightarrow 2_2^+$	0.247	2.84×10^{-3}	3.76×10^{-1}	7.53×10^{-5}	4.22×10^{-4}	15	22(3)
	$3_1^+ \rightarrow 4_1^+$	0.197	2.23×10^{-3}	1.07×10^{-1}	2.96×10^{-5}	3.77×10^{-5}	2.0	1.7[a]
	$5_1^+ \rightarrow 3_1^+$	0.516	0	2.86×10^{-1}	0	1.27×10^{-2}	100	100[a]
	$5_1^+ \rightarrow 4_1^+$	0.712	1.28×10^{-3}	9.22×10^{-3}	8.13×10^{-4}	2.06×10^{-3}	23	18[a]
	$5_1^+ \rightarrow 4_2^+$	0.291	4.26×10^{-3}	1.49×10^{-1}	1.83×10^{-4}	3.73×10^{-4}	4.4	4.2[a]
	$6_2^+ \rightarrow 4_1^+$	1.021	0	8.66×10^{-4}	0	1.18×10^{-3}	4	-
	$6_2^+ \rightarrow 4_2^+$	0.600	0	3.47×10^{-1}	0	3.29×10^{-2}	100	100[a]
	$6_2^+ \rightarrow 5_1^+$	0.309	1.20×10^{-4}	9.56×10^{-3}	6.23×10^{-6}	3.29×10^{-5}	0.1	8[a]
	$6_2^+ \rightarrow 6_1^+$	0.446	4.53×10^{-3}	1.15×10^{-1}	7.07×10^{-4}	2.47×10^{-3}	10	10[a]
	$7_1^+ \rightarrow 5_1^+$	0.645	0	3.85×10^{-1}	0	5.25×10^{-2}	100	100[a]
	$7_1^+ \rightarrow 6_1^+$	0.782	1.88×10^{-3}	1.65×10^{-3}	1.58×10^{-3}	5.88×10^{-4}	5	-
	$7_1^+ \rightarrow 6_2^+$	0.336	6.82×10^{-3}	8.50×10^{-2}	4.55×10^{-4}	4.44×10^{-4}	2	-
	$8_2^+ \rightarrow 6_1^+$	1.159	0	3.12×10^{-3}	0	8.00×10^{-3}	10	-
	$8_2^+ \rightarrow 6_2^+$	0.713	0	3.46×10^{-1}	0	7.78×10^{-2}	100	100[a]
	$9_1^+ \rightarrow 7_1^+$	0.756	0	4.25×10^{-1}	0	1.28×10^{-1}	100	100[a]
	$9_1^+ \rightarrow 8_1^+$	0.833	2.20×10^{-3}	1.06×10^{-5}	2.23×10^{-3}	5.13×10^{-6}	2	-
	$9_1^+ \rightarrow 8_2^+$	0.379	1.38×10^{-2}	5.76×10^{-2}	1.32×10^{-3}	5.48×10^{-4}	1	-
	$10_1^+ \rightarrow 8_1^+$	0.814	0	5.24×10^{-1}	0	2.28×10^{-1}	100	100[a]
	$10_1^+ \rightarrow 8_2^+$	0.360	0	7.45×10^{-3}	0	5.49×10^{-5}	0	-
112	$3_1^+ \rightarrow 2_1^+$	0.511	5.00×10^{-4}	2.07×10^{-2}	1.17×10^{-4}	8.71×10^{-4}	100	100[a]
	$3_1^+ \rightarrow 2_2^+$	0.224	3.57×10^{-3}	3.17×10^{-1}	7.06×10^{-5}	2.18×10^{-4}	29	38[a]
	$3_1^+ \rightarrow 4_1^+$	0.102	2.63×10^{-3}	9.99×10^{-2}	4.91×10^{-6}	1.35×10^{-6}	0.6	-
	$5_1^+ \rightarrow 3_1^+$	0.488	0	2.42×10^{-1}	0	8.07×10^{-3}	100	100[a]
	$5_1^+ \rightarrow 4_1^+$	0.590	1.05×10^{-3}	5.74×10^{-3}	3.80×10^{-4}	5.01×10^{-4}	12	8[a]
	$6_2^+ \rightarrow 4_1^+$	0.925	0	2.05×10^{-3}	0	1.70×10^{-3}	7	-
	$6_2^+ \rightarrow 4_2^+$	0.590	0	2.76×10^{-1}	0	2.41×10^{-2}	100	-
	$6_2^+ \rightarrow 5_1^+$	0.335	9.00×10^{-4}	1.06×10^{-4}	5.96×10^{-5}	5.46×10^{-7}	0	-
	$6_2^+ \rightarrow 6_1^+$	0.380	5.90×10^{-3}	1.04×10^{-1}	5.70×10^{-4}	1.01×10^{-3}	6	-
	$7_1^+ \rightarrow 5_1^+$	0.606	0	3.21×10^{-1}	0	3.17×10^{-2}	100	100[a]
	$7_1^+ \rightarrow 6_1^+$	0.651	1.24×10^{-3}	4.27×10^{-4}	6.02×10^{-4}	6.09×10^{-5}	2	-
	$7_1^+ \rightarrow 6_2^+$	0.271	1.07×10^{-2}	7.67×10^{-2}	3.71×10^{-4}	1.34×10^{-4}	2	-
	$8_2^+ \rightarrow 6_1^+$	1.074	0	7.11×10^{-3}	0	1.22×10^{-2}	26	-
	$8_2^+ \rightarrow 6_2^+$	0.693	0	2.45×10^{-1}	0	4.78×10^{-2}	100	100[a]
	$9_1^+ \rightarrow 7_1^+$	0.694	0	3.36×10^{-1}	0	6.62×10^{-2}	100	100[a]
	$9_1^+ \rightarrow 8_1^+$	0.696	7.30×10^{-4}	7.43×10^{-4}	4.33×10^{-4}	1.48×10^{-4}	1	-
	$9_1^+ \rightarrow 8_2^+$	0.272	1.96×10^{-2}	5.42×10^{-2}	6.94×10^{-4}	9.85×10^{-5}	1	-
	$10_1^+ \rightarrow 8_1^+$	0.723	0	3.92×10^{-1}	0	9.44×10^{-2}	100	100[a]
	$10_1^+ \rightarrow 8_2^+$	0.300	0	1.45×10^{-2}	0	4.22×10^{-5}	0	-

TABLE VII. Experimental $\log ft$ values for the $\beta^{\pm}$ branching to the three lowest 2^+ levels in $^{98-102}$Ru. Experimental data are from [29–31].

		$\log ft$		
Parent nucleus	Daughter nucleus	2_1^+	2_2^+	2_3^+
^{98}Rh; $(2)^+$	^{98}Ru	5.411(13)	6.56(11)	5.62(4)
^{100}Tc; 1^+	^{100}Ru	6.5(4)	7.1(3)	6.5(1)
^{102}Tc; 1^+	^{102}Ru	5.99(6)	~7.0	5.87(6)

lations, both the 8_1^+ and 8_2^+ states have large MS components. The model predicts in this nucleus the existence of just one $J^{\pi}=10^+$ state which is obviously fully symmetric as only five bosons are available. On the basis of the calculated excitation energies, which on average reproduce the experimental ones in this nucleus to better than 3%, it is probably to be identified with the level at 4220 keV. In this hypothesis, the observed branching ratio to the 8_1^+ and 8_2^+ states (85/100) is well reproduced (see Table VI), which fact would hardly be possible if either of the 8^+ states had a pure FS character.

Also the decay properties of the 8_2^+ state in ^{104,108,110,112}Ru are reasonably reproduced by the calculations (see Tables III and VI).

In ^{100,102}Ru the yrast 10^+ state turns out to have a pure MS character, whereas it has a predominant FS character in the heavier nuclei. The absence of experimental data on the decay properties of these states do not allow us to confirm or to contradict the predictions of the model. If these were borne out by the experiment, some revision in the standard backbending plot relative to the g.s. band [47] might be necessary.

B. Odd-spin states

As noted above [see Fig. 5(c)], the calculations suggest for the 3_1^+ level in the lighter nuclei (^{98,100,102}Ru) a structure close to that of the $2d$-boson 3^+ MS state in the U(5) limit of the IBA-2 model. In this limit it is allowed to decay to the $1d$-boson 2_1^+ state through an $E2$ transition and to the $2d$-boson 2_2^+ and 4_1^+ states through transitions dominated by the $M1$ component. The observed branching ratio of the 3_1^+ level in these nuclei is correctly reproduced (see Table VI) due to the predominant $M1$ component found in the $3_1^+\rightarrow 2_2^+$ and $3_1^+\rightarrow 4_2^+$ transitions and to the strong cancellation which occurs for the $E2$ component in the $3_1^+\rightarrow 2_1^+$ transition. For example, in ^{98}Ru the calculations give $\langle \hat{T}_{\nu}(E2;3_1^+\rightarrow 2_1^+)\rangle=-2.46$ and $\langle \hat{T}_{\pi}(E2;3_1^+\rightarrow 2_1^+)\rangle=2.65$. These values are comparable in magnitude to those computed for the $2_1^+\rightarrow 0_1^+$ transition, namely 2.30 and 3.22, respectively. As a further check of the consistency of our interpretation of the 3_1^+ level, we remark that the computed values for the ratio $B(M1;3_1^+\rightarrow 2_2^+)/B(M1;3_1^+\rightarrow 4_1^+)$ are 1.17, 1.35 and 1.25 for ^{98,100,102}Ru, respectively, which are quite close to the ratio 1.33 valid for the U(5) limit [16].

The importance of the MS component in the 3_1^+ state for reproducing the experimental values of δ is illustrated in Fig. 9 where the calculated values of $\delta(3_1^+\rightarrow 2_1^+)$ and $\delta(3_1^+\rightarrow 2_2^+)$ in ^{98}Ru are displayed as a function of ξ_2 (upper part) and ξ_3 (lower part). By taking into account how the $F=F_{\max}$ com-

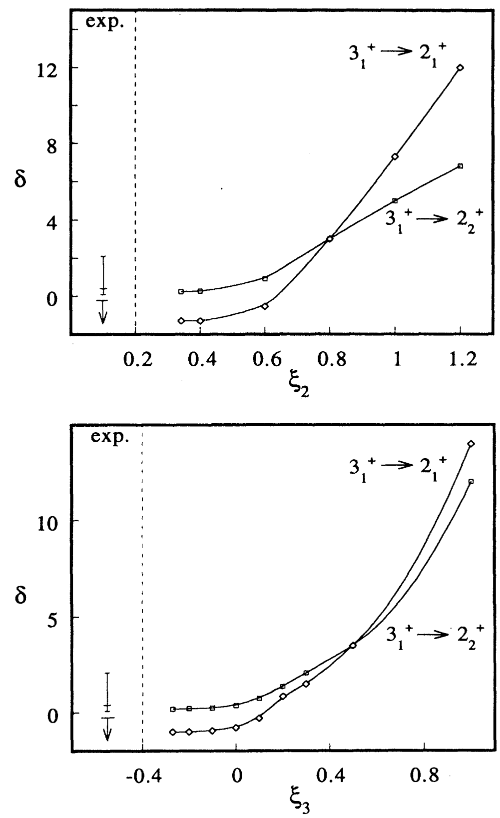

FIG. 9. Calculated values of the $E2/M1$ mixing ratios for the transitions $3_1^+\rightarrow 2_1^+$ and $3_1^+\rightarrow 2_2^+$ in ^{98}Ru as a function of the Majorana parameter ξ_3. The remaining Hamiltonian parameters are those given in Table I. The experimental value for the $3_1^+\rightarrow 2_2^+$ transition together with the upper limit, marked by an arrow, for the $3_1^+\rightarrow 2_1^+$ transition is reported on the left.

ponent of the 3_1^+ level depends on these parameters (see Fig. 3), it is clear that the calculated values of δ are compatible with the experimental ones only if the 3_1^+ level has a large MS component.

The structure of the 3_1^+ level is gradually changing in the heavier isotopes, as shown in Fig. 5(c). For example, in ^{104}Ru, $W_{\gamma}(M1;3_1^+\rightarrow 2_2^+)$ and $W_{\gamma}(M1;3_1^+\rightarrow 4_1^+)$ become comparable to $W_{\gamma}(E2;3_1^+\rightarrow 2_2^+)$ and $W_{\gamma}(E2;3_1^+\rightarrow 4_1^+)$. Since the $B(E2)$ values for the transitions deexciting the 3_1^+ level in this nucleus are well reproduced by the calculations (see Table III) from the observed agreement with the experimental branching ratios and mixing ratios $\delta(3_1^+\rightarrow 2_1^+)$, it follows that also the $M1$ component is correctly predicted.

In the heavier isotopes both the branching ratios from the 3_1^+ level and $\delta(3_1^+\rightarrow 2_1^+)$ are very well reproduced so that one can reasonably assume that even in these nuclei the structure of the 3_1^+ is correctly described by the model.

As to MS states having $J^{\pi}=5^+,7^+,9^+$, they are predicted by the model to be yrast in all isotopes of the chain. Experimental information on the 5_1^+ state is available in ^{102,104,108,110,112}Ru. In the lighter nuclei this state is predicted to be an almost pure MS state containing $3d$ bosons. This is confirmed in ^{102}Ru by the observed branching ratios from the 5_1^+ state to the 3_1^+, 4_2^+, 6_1^+ states. Indeed, the strongest branch populates the 3_1^+ state which has MS character and the sizable branchings to the 4_2^+, 6_1^+ levels, which have essentially a $3d$-boson FS structure, are successfully reproduced by the calculations just for the presence of a predominant $M1$ component in the corresponding transitions. We also observe that the mixing ratio $\delta(5_1^+ \rightarrow 4_1^+)$ is well reproduced. In heavier isotopes the branching ratios from the 5_1^+ level are also quite successfully predicted by the model.

Having established the MS character of the 3_1^+ and 5_1^+ levels, it is easy to recognize the same character for the $J^\pi = 7_1^+, 9_1^+$ levels in ^{108,110,112}Ru, as follows from the highly preferential decay of these levels to the final state of spin $J_f = J_i - 2$. This would certainly not be the case if the initial and final level had a different symmetry character. We conclude therefore that the observed decay properties confirm the MS character of the odd-spin yrast states displayed in Fig. 5(c).

It follows from our analysis that, in nuclei of this mass region, the order of magnitude of $B(M1)$ for transitions connecting MS and FS states having large components with the same d-boson number ("allowed" transitions) is about $10^{-2}\mu_N^2$.

V. CONCLUSIONS

As a part of a systematic investigation aimed at identifying states having a large mixed-symmetry component in the mass region $A = 100-120$, we have analyzed, in the framework of the IBA-2 model, the isotopic chain of even ruthenium isotopes $^{98-114}$Ru. The parameters of the Hamiltonian were optimized by comparison with available experimental data on the excitation energy of low-lying positive parity levels up to spin $J = 10$. It turns out that a good overall agreement between calculated and observed excitation patterns can only be achieved by taking into account the presence, at rather low energy, of states having a large MS component. The crucial importance of the values of the Majorana parameters in achieving such a result has been repeatedly stressed. In particular, we succeeded in restricting the range of "reasonable" values for the parameters ξ_2 and ξ_3, which can constitute a useful starting point for a similar analysis in the whole $A = 100-120$ mass region. The decay properties of the relevant levels have been compared to the predictions of the model taking into account all the available experimental data on static and transition electric quadrupole and magnetic dipole moments as well as mixing and branching ratios. Apart for a few discrepancies, a satisfactory general account of the decay properties of positive parity levels up to $J^\pi = 10^+$ has been obtained. In particular, the model is able to reproduce the properties of the first excited 0_2^+ state which in the past has been considered as an intruder state. A large body of evidence for assigning to several levels an MS character has been collected. The lowest ones appear to be the 2_3^+ and 3_1^+ levels. This finding is in agreement with the identification of the 2_3^+ state as the lowest state having MS character in ^{110,112,114}Cd isotopes [21]. Sizable MS components seem to be present in the 6_2^+ and 8_2^+ levels. Particularly interesting is the presence, above the 3_1^+ level, of a band of states having $J^\pi = 5^+$, 7^+, and 9^+ which possess a large MS component at least in the heavier nuclei of the chain.

In this work, an analysis in search of MS states has been performed systematically along an isotopic chain and has not been limited to the lowest-lying states. The smooth variation of the properties of levels identified as basically MS states as a function of the mass number strongly supports their interpretation in term of a collective model.

The lack of experimental data on spin, parity, and lifetime of many low-lying levels as well as on $E2/M1$ mixing ratios of several transitions has prevented us from performing a more extended comparison. We hope to be able to measure some of these quantities in the near future.

[1] A. Arima, T. Otsuka, F. Iachello, and I. Talmi, Phys. Lett. **66B**, 205 (1977).

[2] T. Otsuka, A. Arima, F. Iachello, and I. Talmi, Phys. Lett. **76B**, 139 (1978).

[3] T. Otsuka, A. Arima, F. Iachello, Nucl. Phys. **A309**, 1 (1978).

[4] F. Iachello, Phys. Rev. Lett. **53**, 1427 (1984).

[5] F. Iachello and A. Arima, *The Interacting Boson Model* (Cambridge University Press, Cambridge, 1987).

[6] I. Talmi, *Simple Model of Complex Nuclei* (Harwood Academic Publishers, Switzerland, 1993).

[7] A. B. Balantekin, B. R. Barrett, and S. Levit, Phys. Lett. **129B**, 153 (1983).

[8] A. B. Balantekin and B. R. Barrett, Phys. Rev. C **32**, 288 (1985).

[9] A. B. Balantekin and B. R. Barrett, Phys. Rev. C **33**, 1842 (1986).

[10] O. Scholten, K. Heyde, P. Van Isacker, J. Jolie, J. Moreau, M. Waroquier, and J. Sau, Nucl. Phys. **A438**, 41 (1985).

[11] P. Van Isacker, K. Heyde, J. Jolie, and A. Sevrin, Ann. Phys. **171**, 253 (1986).

[12] A. B. Balantekin, B. R. Barrett, and P. Halse, Phys. Rev. C **38**, 1392 (1988).

[13] A. B. Balantekin and B. R. Barrett, Phys. Rev. C **35**, 187 (1987).

[14] C. De Coster and K. Heyde, Int. J. Mod. Phys. A **4**, 3907 (1989).

[15] B. R. Barrett and T. Otsuka, Phys. Rev. C **42**, 2438 (1990); **46**, 1735 (1992).

[16] A. Giannatiempo, G. Maino, A. Nannini, and P. Sona, Phys. Rev. C **48**, 2657 (1993).

[17] D. Böhle, A. Richter, W. Steffen, A. E. L. Dieperink, N. Lo Iudice, F. Palumbo, and O. Scholten, Phys. Lett. **137B**, 27 (1984).

[18] P. O. Lipas, P. von Brentano, and A. Gelberg, Rep. Prog. Phys. **53**, 1353 (1990).

[19] J. H. Hamilton, Nucl. Phys. **A520**, 377C (1990).

[20] S. T. Ahmad, W. D. Hamilton, P. Van Isacker, S. A. Hamada, and S. J. Robinson, J. Phys. G **15**, 93 (1989).

[21] A. Giannatiempo, A. Nannini, A. Perego, P. Sona, and G. Maino, Phys. Rev. C **44**, 1508 (1991).

[22] A. Giannatiempo, A. Nannini, A. Perego, and P. Sona, Phys. Rev. C **44**, 1844 (1991).

[23] A. Giannatiempo, A. Nannini, P. Sona, and D. Cutoiu, 5th International Spring Seminar on New Perspectives in Nuclear

Structure, Ravello, 1995, unpublished.
[24] J. Stachel, P. Van Isacker, and K. Heyde, Phys. Rev. C **25**, 650 (1982).
[25] R. F. Casten and D. D. Warner, Rev. Mod. Phys. **60**, 389 (1988).
[26] P. van Isacker and G. Puddu, Nucl. Phys. **A348**, 125 (1980).
[27] T. Otsuka, N. Yoshida, Program NPBOS Japan Atomic Energy Research Institute Report JAERI-M85-094, 1985.
[28] O. Scholten, K. Heyde, P. Van Isacker, and T. Otsuka, Phys. Rev. C **32**, 1729 (1985).
[29] O. Scholten, Ph.D. thesis, University of Groningen, 1980, unpublished.
[30] T. Otsuka, Nucl. Phys. **A557**, 531 (1993).
[31] B. Singh, Nucl. Data Sheets **67**, 693 (1992).
[32] B. Singh and J. A. Szucs, Nucl. Data Sheets **60**, 1 (1990).
[33] D. De Frenne and E. Jacobs, Nucl. Data Sheets **63**, 373 (1991).
[34] J. Blanchot, Nucl. Data Sheets **64**, 1 (1991).
[35] D. De Frenne and E. Jacobs, Nucl. Data Sheets **53**, 73 (1988).
[36] J. Blanchot, Nucl. Data Sheets **62**, 803 (1991).
[37] D. De Frenne and E. Jacobs, Nucl. Data Sheets **67**, 809 (1992).
[38] D. De Frenne, E. Jacobs, and M. Verboven, Nucl. Data Sheets **57**, 443 (1989).
[39] J. Stachel, N. Kaffrell, E. Grosse, H. Emling, H. Folger, R. Kulessa, and D. Schwalm, Nucl. Phys. **A383**, 429 (1982).
[40] J. Stachel *et al.*, Nucl. Phys. **A419**, 589 (1984).
[41] J. L. Durell, in *Proceedings of the International Conference on the Spectroscopy of Heavy Nuclei*, Crete, 1989, edited by J. F. Sharpey-Schafer and L. Skouras, Institute of Physics Conference Series 105 (IOP, London, 1990).
[42] J. A. Shannon *et al.*, Phys. Lett. B **336**, 136 (1994).
[43] J. Äystö *et al.*, Nucl. Phys. **A515**, 365 (1990).
[44] A. Giannatiempo, A. Nannini, A. Perego, P. Sona, and D. Cutoiu, unpublished.
[45] W. D. Hamilton, J. Phys. G **16**, 745 (1990).
[46] F. Iachello, in *Proceedings of the International Conference on Perspectives for the Interacting Boson Model on the Occasion of its 20th Anniversary,* Padua, 1994, edited by R. F. Casten *et al.* (World Scientific, Singapore, 1994).
[47] Y. Abdelrahman, J. L. Durell, J. B. Fitzgerald, M. A. C. Hotchkis, A. S. Mowbray, W. R. Phillips, and B. J. Varley, Daresbury Annual report 1988/89, p. 11.